# Critical factors affecting the amorphous phase formation of NiTiZrSiSn bulk amorphous feedstock in vacuum plasma spray

HANSHIN CHOI*
*Nano Material Team, Korea Institute of Industrial Technology, Incheon 404-254, Korea*

JUNESEOB KIM, CHANGHEE LEE
*Division of Materials Science & Engineering College of Engineering, Hanyang University, 17 Haengdang-dong, Seongdong-ku, Seoul 133-791, Korea*

KOO HYUN LEE
*Korean Institute of Machines and Materials, Changwon, 614-010, Korea*

Amorphous metallic materials show very attractive properties in engineering points such as friction, wear, and corrosion resistance [1–3]. Moreover, a lot of bulk metallic glass [BMG] materials with much improved glass forming ability [GFA] have been developed [4]. Higher GFA can enlarge the applications of BMGs in industries. From the practical point of view, overlying BGMs as protective coatings onto cheap structural materials is more effective considering the limited plasticity. In the thermal spraying coating process [5], cooling rate of the impacting particle is generally up to $10^5$ $Ks^{-1}$, while the critical cooling rates for amorphous phase formations of Zr-base, Fe-base, Co-base, and Ni-base bulk amorphous alloys are reduced to be lower than $10^2$ $Ks^{-1}$ [6]. However, in-flight particle oxidation during atmospheric plasma spraying [APS] and high-velocity oxy-fuel [HVOF] spraying was inevitable due to the turbulent nature of the plasma jet in the APS process and the presence of free oxygen arising from incomplete combustion of fuel gas in the HVOF process mentioned in our other works [7]. As a matter of fact, preferential oxidation of Zr and Ti in an in-flight particle triggered the destabilization of the bulk metallic glass particle because amorphous phase stability and formability are largely affected by the chemical composition-dependent critical cooling rate. So the vacuum plasma spraying process was chosen for the formation of a NiTiZrSiSn bulk amorphous coating because the powder is very sensitive to oxidation. The effects of the plasma gas composition on the impacting particle energy state and the resulting phase composition were investigated in this study.

A bulk amorphous NiTiZrSiSn powder was produced using inert gas atomization. It was sprayed onto the pre-treated copper substrate using a vacuum plasma spraying system under the processing parameters as summarised in Table I. In order to change the thermal energy of in-flight particles, hydrogen gas flow rate in the plasma gas mixture was changed. As the hydrogen gas flow rate was increased, the arc power was increased owing to the increase of arc voltage. In addition, the thermal conductivity of the plasma jet is also increased. Accordingly, thermal energy of in-flight particle is increased due to the enhanced gas enthalpy and thermal conductivity considering the heat transfer reaction in thermal plasma spraying. In fact, the effects of hydrogen gas flow were empirically confirmed using DPV-2000 in the atmospheric plasma spraying process of alumina–titania feedstock in our other work [8].

As shown in Fig. 1, a halo diffuse peak with sharp crystalline peaks could be observed regardless of the composition of the plasma gas mixture within the scope of this study. However, the sharp peak intensities from the crystallisation of in-flight amorphous particles generally decrease with the increase of the hydrogen gas flow rate except for the V1 coating. The crystalline phases present in the as-sprayed coatings were cubic Ni(Ti,Zr) and orthorhombic $Ni_{10}(Ti,Zr)_7$ intermetallic compounds. Note that Cu-crystalline peaks were also observed in V1 coating: when the cross section was observed, continuous overlapping did not occur in V1 coating. Plane-view morphologies of the as-sprayed VPS NiTiZrSiSn coatings can be seen in Fig. 2. All kinds of splat morphologies which are encountered in thermal spraying process are present on the as-sprayed

TABLE I Process parameters

| Desig. | H2 gas flow rate | Arc voltage (V) | Arc power (kw) | Water power (kw) | Gun efficiency (%) | Net power [kw] |
|---|---|---|---|---|---|---|
| V1 | 4slm | 49 | 24.5 | 12.6 | 49 | 11.9 |
| V2 | 6slm | 53 | 26.5 | 13.0 | 51 | 13.5 |
| V3 | 8slm | 57 | 28.5 | 13.8 | 52 | 14.7 |
| V4 | 10slm | 61 | 30.5 | 15.0 | 51 | 15.5 |

Invariables

| | | | |
|---|---|---|---|
| Arc current | 500 A | Feeding rate | 45 $gm^{-1}$ |
| Spraying distance | 250 mm | Initial chamber pressure | $5 \times 10^{-4}$ bar |
| | | Working pressure | 0.25 bar |
| Argon gas flow rate | 40 slm | Plasmatron travel rate | 1 $ms^{-1}$ |

slm: Standard litre per minute.

*Author to whom all correspondence should be addressed.

  

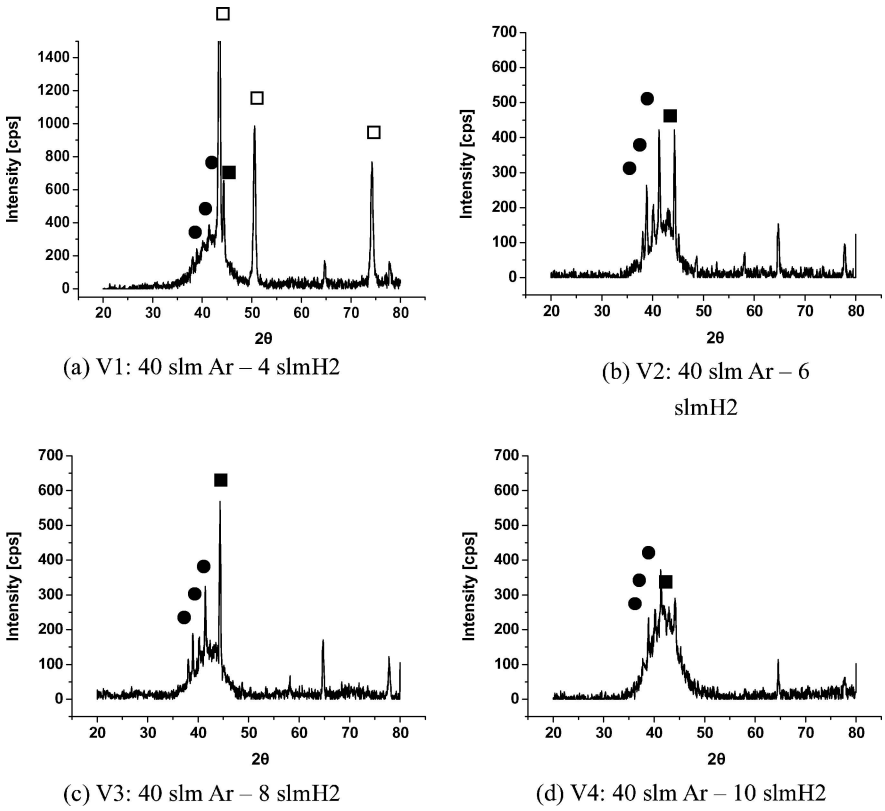


*Figure 1* X-ray diffraction of the as-sprayed coating according to the hydrogen gas flow rate. [□: Cu, ■: $Ni_{10}(Ti,Zr)_7$, and ●: Ni(Ti,Zr)]

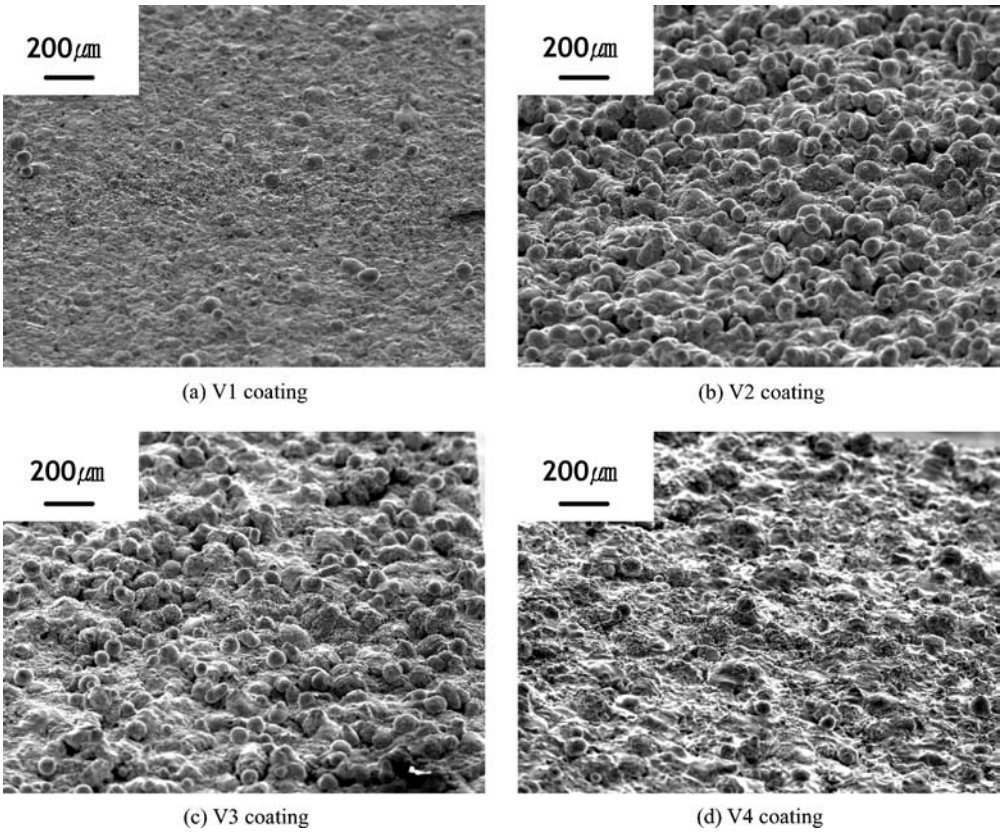


*Figure 2* Plane-view morphology of as-sprayed coating according to plasma gas composition.

coating surface: well-shaped disc-like splats and highly splashed splats are from the deposition of fully melted particles, while spherical particles on the coat surface result from that of unmelted part in a partially melted one. Similar to the X-ray diffraction, hydrogen gas flow rate has a critical influence on both unmelted spherical particle number density and size also, except for the V1 coating. In view of the interaction between in-flight particles and the thermal plasma jet, the increase of the unmelted particle number density in the as-sprayed

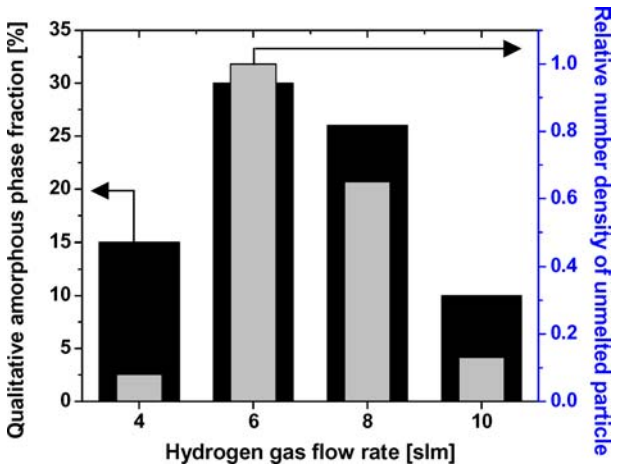


*Figure 3* Qualitative crystalline phase fraction according to hydrogen gas flow rate.

coating resulted from the lower gas enthalpy and thermal conductivity at the reduced hydrogen gas flow rate. For the qualitative comparison, area fraction of the crystalline phase peaks was calculated: in the case of V1 coating, overlapped peaks from copper substrate were not considered in the calculation. Also, the unmelted particle number density at the same detecting area of 4 $mm^2$ was measured using an image analysis. Except for the V1 coating, both qualitative crystalline phase fraction and unmelted particle number density were decreased with the increase of the hydrogen gas flow rate as can be seen in Fig. 3. Through these results, it could be deduced that the crystalline peaks in the coating resulted from the presence of unmelted part of partially melted splat in the coating.

In the case of the V1 coating, the melting degree and the resulting amorphous phase fraction were apparently improved. However, qualitative deposition efficiency estimated by the coating thickness was the lowest and the splat size and unmelted particle size were also the smallest. It means that most of the impacting particles did not obtain a sufficient melting degree enough to deposit at the moment of impact. Also large particles did not melt effectively during flight since the heating rate decreased with the increase of the particle size. Thus, both the decrease of unmelted particle size with the increase of hydrogen gas flow rate and the fine unmelted particle size in V1 coating are rational. From the viewpoint of the metallurgical properties of the bulk amorphous feedstock, thermal energy including temperature and melting degree of an in-flight bulk amorphous powder had a critical influence on the phase evolution. When the particle was heated above the melting temperature, liquid droplets solidified to the amorphous phase during the VPS process. However, the crystallized particles remained in the coating if the particles were heated to a temperature between the crystallization temperature and melting temperature owing to the irreversible solid-state crystallization.

Through this study, the amorphous phase fraction of the VPS NiTiZrSiSn coating was found to be primarily dependent on the in-flight particle melting degree. As the particle melting degree increased, the amorphous phase fraction also increased. Also, the increase of the hydrogen gas flow rate improved the degree of in-flight particle melting.

## Acknowledgements

We acknowledge that this research was performed using the financial support provided by MOICE(Ministry of Commerce, Industry, and Energy) under the project named development of structural metallic materials and parts with super strength and high performance.

## References

1. K. KISHITAKE, H. ERA and F. OTSUBO, *J. Thermal Spray Technol.* **5** (1996) 476.
2. A. KAWASHIMA, H. HABAZAKI and K. HASHIMOTO, *Mater. Sci. Eng.* **A304-306** (2001) 753.
3. F. E. LUBORSKY *et al.*, Amorphous Metallic Alloys, edited by F. E. Luborsky (1983) p. 1.
4. A. INOUE, *Mater. Sci. Eng.* **A304–306** (2001) 1.
5. R. B. HEIMANN, Plasma Spray Coating: Principles and Applications (VCH, New York, 1996) p. 993.
6. A. INOUE, *Acta Mater.* **48** (2000) 279.
7. H. CHOI, S. LEE, B. KIM and C. LEE, *J. Non-Cryst. Solids*, in preparation.
8. H. CHOI, H. YANG, C. LEE and S. HWANG, *Thin Solid Films*, in-revised.

*Received 15 January*
*and accepted 12 August 2004*